AIMS Bioengineering, 4(1): 162-170.
DOI: 10.3934/bioeng.2017.1.162
Received: 13 January 2017
Accepted: 21 February 2017
Published: 28 February 2017

http://www.aimspress.com/journal/Bioengineering

Research article

Effect of nanometer scale surface roughness of titanium for osteoblast function

Satoshi Migita * and Kunitaka Araki

Graduate School of Science and Engineering, Yamagata University, 4-3-16 Jonan, Yonezawa, Yamagata 992-8510, Japan

* **Correspondence:** Email: migita@yz.yamagata-u.ac.jp; Tel: +8-123-826-3740.

Abstract: Surface roughness is an important property for metallic materials used in medical implants or other devices. The present study investigated the effects of surface roughness on cellular function, namely cell attachment, proliferation, and differentiation potential. Titanium (Ti) discs, with a hundred nanometer- or nanometer-scale surface roughness (rough and smooth Ti surface, respectively) were prepared by polishing with silicon carbide paper. MC3T3-E1 mouse osteoblast-like cells were cultured on the discs, and their attachment, spreading area, proliferation, and calcification were analyzed. Cells cultured on rough Ti discs showed reduced attachment, proliferation, and calcification ability suggesting that the surface inhibited osteoblast function. The findings can provide a basis for improving the biocompatibility of medical devices.

Keywords: titanium; roughness; osteoblast; cell attachment; biomaterial

1. Introduction

Metallic biomaterials, such as titanium (Ti) and its alloys, are widely used in clinical applications, including in dental implants, artificial hip joints, and bone and external fixator [1,2]. The surface of these devices is often modified to improve biocompatibility [3,4,5]. Surface roughening is particularly effective for improving biocompatibility and inducing osseointegration [6,7]. For example, it has been demonstrated that surfaces treated by sand blasting and alkaline etching (SLA), a major technique for creating a roughened surface improves hard tissue compatibility [8], and micro-arc anodic oxidation, MAO yields a roughened surface for providing good corrosion resistance and biocompatibility [9,10,11]. On the other hand, excessively strong

binding between bone and Ti can lead to refracture after remove the devices [12,13]; which can be prevented by inhibiting bone callus formation on the Ti surface [14].

There are various reports regarding the effect of roughness on cell behaviors such as proliferation and differentiation. Ti with micrometer-scale average surface roughness (Ra) exhibited greater cell attachment than Ti with a smooth surface [15]. Osteoblast proliferation and differentiation were also shown to be increased by micrometer-scale Ra [16,17]. In contrast, Ti with nanometer-scale Ra had no effect on osteoblast function [18]. We previously reported that Ti surfaces with Ra in the order of 100 nm markedly reduced fibroblast attachment and proliferation [19]. Although these cells formed retained their characteristic morphology, there was little spreading. Cell morphology is closely related to cellular function through cell adhesion and membrane tension [20,21,22].

In the present study, we investigated whether 100 nm-scale surface roughness influences osteoblast function. We prepared roughened Ti surfaces with a range of Ra values using silicon carbide (SiC) paper, which did not influence the chemical composition of the passive film on the Ti surface. Osteoblast were cultured on the surfaces and their adhesion, proliferation, and calcification were evaluated. The results insight into interaction between cells and materials as well as a basis for inhibiting bone callus formation on Ti implants and thus preventing refracture after nail extraction.

2. Materials and Method

2.1. Preparation of substrates

Commercially sourced pure Ti (Rare Metallic Co., Tokyo, Japan) were mirror-polished. To roughen the surface, they were then repolished with SiC paper and rinsed by sonication in acetone, methanol, and Milli-Q water. Before cell culture, the Ti discs were sterilized with 70% ethanol for 1 h under ultraviolet light. The surface of Ti discs was visualized with a scanning probe microscope (SPM-9600; Shimadzu, Kyoto, Japan) using a silicon cantilever (NCHR-20; Nano world AG, Neuchâtel Switzerland). Ra were automatically calculated by examining Z-range images.

2.2. Protein adsorption

Bovine serum albumin (BSA; Thermo Fisher Scientific, Waltham, MA, USA) was dissolved in 0.1 M phosphate-buffered saline (PBS; Takara Bio, Otsu, Japan) at a concentration of 1 mg/ml. Ti discs were immersed in the protein solution at 37 °C for 1 h. Proteins adsorbed on the Ti were removed by sonication in 5% sodium dodecyl sulfate (Wako pure chemical, Osaka, Japan) and quantified with the micro bicinchoninic acid (micro-BCA) assay (Thermo Fisher Scientific). Absorbance at 562 nm was measured with a Smartspec Plus spectrophotometer (Bio-Rad, Hercules, CA, USA).

2.3. Analysis of cell attachment and proliferation

MC3T3-E1 mouse osteoblasts were obtained from Riken Cell Bank (Tsukuba, Japan) and cultured in α-Minimal Essential Medium (Sigma-Aldrich, St Louis, MO, USA) supplemented with 10% fetal bovine serum (Biowest, Nuaillé, France), 100 U/ml penicillin, and 100 μg/ml

streptomycin (Nacalai Tesque, Kyoto, Japan). To evaluate attachment, cells were seeded on substrates at a density of 30,000 cells/cm^2. After 1 or 4 h of incubation, non-adherent cells were removed washing with PBS. Attached cells were quantified using Cell Counting Kit (CCK)-8 (Dojin Chemical, Kumamoto, Japan). To assess proliferation, cells were seeded on Ti discs and tissue culture polystyrene (TCPS) at a density of 5000 cells/cm^2. After 1, 3, 5, and 7 days of culture, the number of cells was quantified with CCK-8.

2.4. Fluorescence microscopy

Integrin α5 expression was visualized by immunocytochemistry. Cells were fixed with 4% paraformaldehyde for 1 h. Nonspecific antibody binding was blocked with SuperBlock (Thermo Fisher Scientific). For integrin α5 labeling, cells were incubated with rat anti-mouse CD49e IgG as a primary antibody followed by fluorescein isothiocyanate-conjugated goat anti-rat IgG secondary antibody (both from Sigma-Aldrich), then visualized by fluorescence microscopy (IX-71; Olympus, Tokyo, Japan). Images were captured with a charge-couple device camera and processed with ImageJ software (http://imagej.nih.gov/ij/).

2.5. Determination of cell spreading analysis

To facilitate visualization, cells were seeded at a density of 3000 cells/cm^2 and cultured in a CO_2 incubator. After 4 h, the cells were stained with calcein-AM (Dojin Chemical) and observed with a fluorescence microscope. Cell spreading area was calculated using ImageJ software.

2.6. Analysis of calcification

Calcification was induced in MC3T3-E1 cells grown on Ti discs by adding 2 mM β-glycerophosphate (Calbiochem, San Diego, CA, USA) and 50 mM ascorbic acid (Wako Pure Chemical) to the culture medium for 7, 14, 21, and 28 days. Calcification level was assessed by Alizarin Red S quantification assay according to following paper [23]. Briefly, cells were fixed with 4% paraformaldehyde at room temperature for 15 min. After rinse with distilled H_2O, the cells were stained with 1% Alizarin Red S solution (adjusted to pH 4.1 with ammonium hydroxide) at room temperature for 30 min. After removing the Alizarin Red S solution, the discs were rinsed twice with distilled H_2O. For quantification Ti discs were immersed in 10% acetic acid for 30 min and the mineralized layer was scraped from the surface, yielding a slurry that was heated at 85 °C for 10 min and then transferred to ice for 5 min. After heating, the slurry was centrifuged at 20,000 × g for 15 min and the supernatant was transferred to a new tube. Ammonium hydroxide (10% v/v) was added to neutralized the acid and the absorbance of the solution at 405 nm was measured.

2.7. Statistical analysis

Five samples (n = 5) were analyzed for each experiment. Differences between groups were evaluated by one-way ANOVA. $P < 0.05$ was considered statistically significant.

3. Results and Discussion

The surface topology of Ti discs with varying degrees of roughness were examined (Figure 1). Ra was measured with an SPM in 20 μm × 20 μm area. Ra values and water contact angles are listed in Table 1; Ra value were 1.8 ± 1.5 nm, and 118.3 ± 1.9 nm and contact angles were 50.8 ± 8.9°, and 56.2 ± 12.4° for Smooth and rough Ti, respectively. The slight difference in contact angle between the two surface was due to roughness, since their surface chemistry was quite similar. The adsorption of BSA on Ti was determined with the micro-BCA assay and was found to be 14.8 ± 2.0 μg and 13.2 ± 2.0 μg for rough and smooth surfaces, respectively (Figure 2). These results suggest that nanometer-scale roughness has minimal effect on the amount of protein adsorbed.

Table 1. Ra and water contact angle of rough and smooth Ti.

	Rough Ti	Smooth Ti
Roughness, Ra (nm)	105.6 ± 1.9	1.8 ± 1.5
Contact angle (degree)	50.8 ± 8.9	56.2 ± 12.4

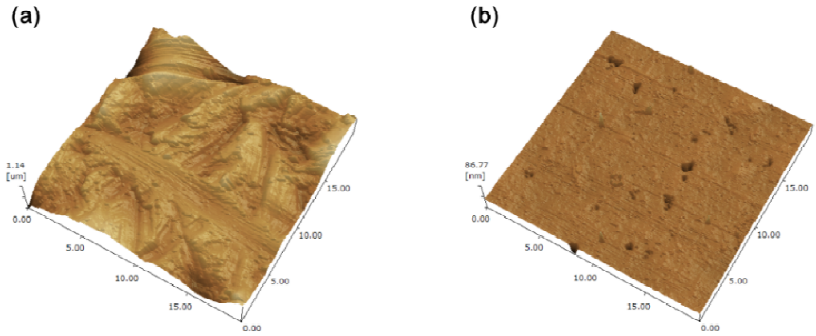

Figure 1. AFM topological images of each substrate. (a) rough and (b) smooth Ti in of 20 μm × 20 μm area.

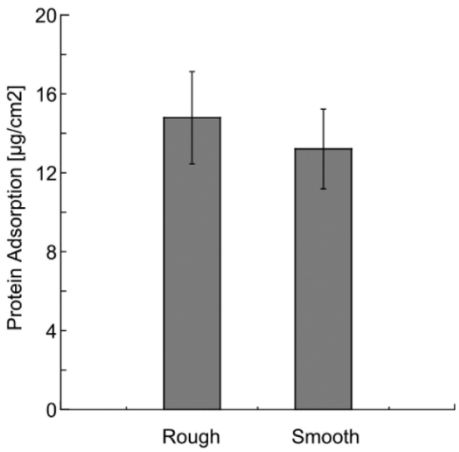

Figure 2. Determination of protein adsorption. Adsorbed bovine serum albumin on rough and smooth were determined by micro-BCA method. Data are the mean ± SD (n = 5).

Cell attachment to the Ti surface was calculated as a percentage of the value for cells attached to TCPS after 1 and 4 h of incubation (Figure 3). The percentage of cells attached to rough and smooth surfaces was 35.6 ± 5.5% and 67.0 ± 4.2%, respectively, after 1 h and 49.2 ± 4.4% and 89.3 ± 5.0%, respectively, after 4 h. More cells were attached to the smooth that to the rough surface. Wettability and protein adsorption data indicated that smooth and the rough Ti had similar chemical composition; hence, the observed difference in cell behavior the two surfaces was attributable to roughness. Cell adhesion to the smooth surface which had a nanometer-scale Ra and to TCPS was similar (data not shown), consistent with findings that nanometer-scale surface roughness had no effect on cellular function [18]. However, the rough surface which had an Ra value in the order of hundreds of nanometer reduced osteoblast attachment, consistent with our previous observations in fibroblasts [19].

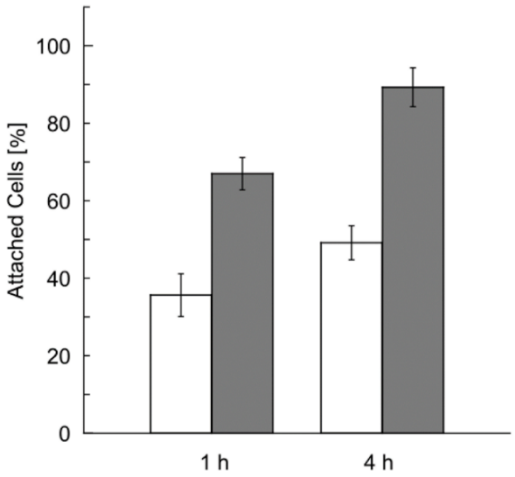

Figure 3. Cell attachment analysis. Attachment activity of cells cultured on the rough Ti (open bar), and smooth Ti (gray bar) for 1 h and 4 h. Data are the mean ± SD (n = 5).

Cell spreading area on rough and smooth Ti surfaces after 4 h of culture according to histogram peaks was 1,900 μm^2 and 5,000 μm^2 for rough and smooth Ti surface, respectively (Figure 4a). Fluorescence micrographs of cells cultured on the two types of surface for 4 h revealed that those on the smooth surface had a spindle-shaped morphology similar to ells grown on TCPS; in contrast, cells on rough Ti had a rounded shape and showed less spreading (Figure 4b). To investigate the potential of Ti discs to act as scaffolds, we visualized integrin α5 expression by fluorescence microscopy (Figure 4c). Cells on the smooth Ti surface showed clear punctae corresponding to integrin α5. Integrin α5 subunit forms heterodimer with β1 subunit and binds Arg-Gly-Asp motif of extracellular matrix (ECM) protein [24]. Thus, the higher degree of cell attachment activity to the smooth Ti surface was achieved via integrin-mediated adhesion. In contrast, there was no distinct integrin α5 expression in cells grown on rough Ti, suggesting that they attach via an integrin independent mechanism, although the rough surface did not induced extensive cell attachment.

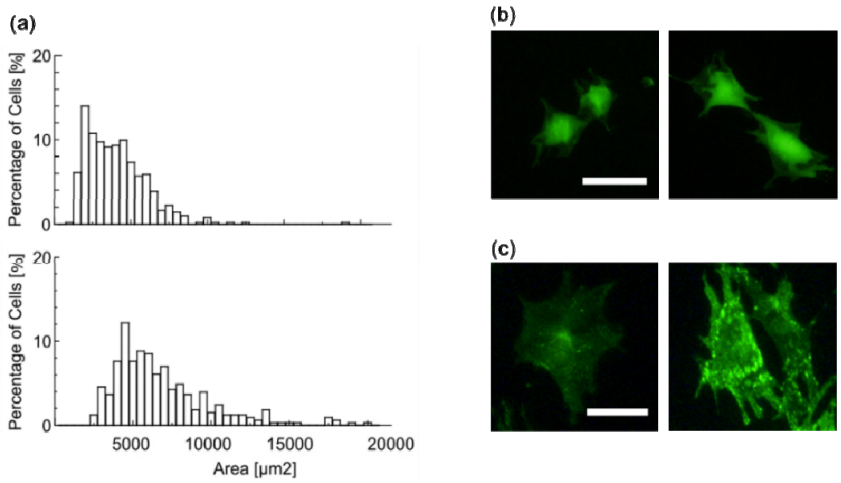

Figure 4. Evaluation of cell adhesion and morphology. (a) Histograms of the cell spreading area of cells cultured on rough Ti (top) and smooth Ti (bottom). (b) Fluorescent microscopic image of cytoplasm stained by calcein-AM of cells cultured on rough Ti (right) and smooth Ti (left). Scale bar = 50 μm. (c) Fluorescent microscopic image of immunostaining of integrin α5 of of cells cultured on rough Ti (right) and smooth Ti (left). Scale bar = 25 μm.

Integrin-ECM complexes generate intracellular signals for cell growth, proliferation, migration, and differentiation [25–28]. To investigate the effect of Ra on cellular function, we compared the proliferation of MC3T3-E1 cells grown on rough and smooth Ti surfaces (Figure 5). Cells on the smooth Ti surface showed similar proliferative capacity to those on TCPS; however, proliferation was inhibited by the rough Ti surface. We also examined calcification of extracellular component as a marker of differentiation capacity. The level of calcification was higher in cells on the smooth as compared to the rough Ti (Figure 6). These results suggest that the latter surface inhibits osteoblast proliferation and differentiation.

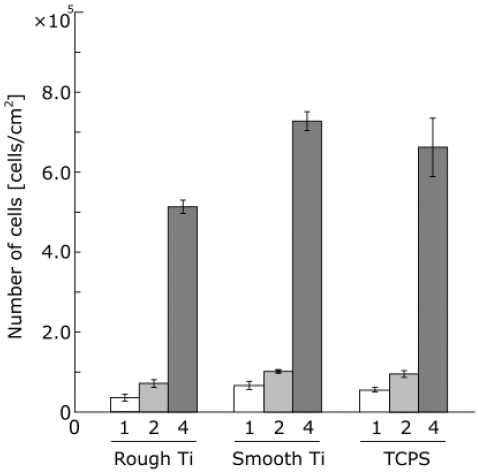

Figure 5. Proliferation of cells cultured on rough Ti and smooth Ti for 1 (open bar), 2 (lightgray bar), and 4 (gray bar) days. Data are the mean ± SD (n = 5).

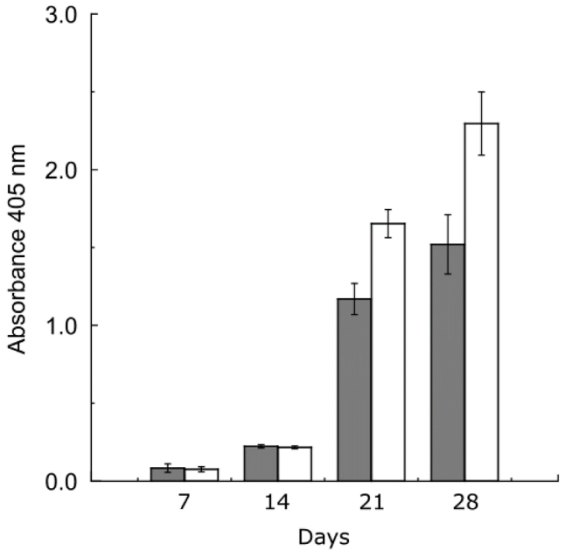

Figure 6. Determination of calcification activity of the cells cultured on rough Ti (open bar) and smooth Ti (gray bar). The cells were induced calcification by ascorbic acid and β-glycerophosphate during 7 to 28 days after seeding. Data are the mean ± SD (n = 5).

4. Conclusion

The results of this study revealed that the rough Ti surface, which had an Ra value in the order of hundreds of nanometers, inhibited cells attachment as well as osteoblast proliferation and differentiation, despite having a similar water contact angle and protein adsorption capacity as the smooth Ti surface. Our findings provide insight into interactions between cells and materials and can be useful for improving the biocompatibility of metallic materials used for medical devices.

Acknowledgments

This work was supported by JSPS KAKENHI Grant-in-Aid for Young Scientists 25820397.

Conflict of Interest

All authors declare no conflicts of interest in this paper

References

1. Williams DF (2009) On the nature of biomaterials. *Biomaterials* 30: 5897–5909.
2. Hanawa T (2012) Research and development of metals for medical devices based on clinical needs. *Sci Technol Adv Mater* 13: 64102–64116.
3. Kirmanidou Y, Sidira M, Drosou ME, et al. (2016) New Ti-alloys and surface modifications to improve the mechanical properties and the biological response to orthopedic and dental implants: a review. *Biomed Res Int* 2016: 2908570–2908590.

4. Mahapatro A (2015) Bio-functional nano-coatings on metallic biomaterials. *Mater Sci Eng C* 55: 227–251.
5. Duraccio D, Mussano F, Faga MG (2015) Biomaterials for dental implants: current and future trends. *J Mater Sci* 50: 4779–4812.
6. Chang PC, Lang NP, Giannobile WV (2010) Evaluation of functional dynamics during osseointegration and regeneration associated with oral implants. *Clin Oral Implan Res* 21: 1–12.
7. Gittens RA, Olivares-Navarrete R, Schwartz Z, et al. (2014) Implant osseointegration and the role of microroughness and nanostructures: lessons for spine implants. *Acta Biomater* 10: 3363–3371.
8. Zhao G, Raines AL, Wieland M, et al. (2007) Requirement for both micron- and submicron scale structure for synergistic response of osteoblasts to substrate surface energy and topography. *Biomaterials* 28: 2821–2829.
9. Zhang RF, Qiao LP, Qu B, et al. (2015) Biocompatibility of micro-arc oxidation coatings developed on Ti6Al4V alloy in a solution containing organic phosphate. *Mater Lett* 153: 77–80.
10. Santiago-Medina P, Sundaram PA, Diffoot-Carlo N (2014) The effects of micro arc oxidation of gamma titanium aluminide surfaces on osteoblast adhesion and differentiation. *J Mater Sci Mater Med* 25: 1577–1587.
11. Wang L, Shi L, Chen J, et al. (2014) Biocompatibility of Si-incorporated TiO_2 film prepared by micro-arc oxidation. *Mater Lett* 116: 35–38.
12. Yao CK, Lin KC, Tarng YW, et al. (2014) Removal of forearm plate leads to a high risk of refracture: decision regarding implant removal after fixation of the forearm and analysis of risk factors of refracture. *Arch Orthop Traum Surg* 134: 1691–1697.
13. Kovar FM, Strasser E, Jaindl M, et al. (2015) Complications following implant removal in patients with proximal femur fractures-an observational study over 16 years. *Orthop Traum Surg Res* 101: 785–789.
14. Takada R, Jinno T, Tsutsumi Y, et al. (2017) Inhibitory effect of zirconium coating to bone bonding of titanium implants in rat femur. *Mater Trans* 58: 113–117.
15. Sammons RL, Lumbikanonda N, Gross M, et al. (2005) Comparison of osteoblast spreading on microstructured dental implant surfaces and cell behaviour in an explant model of osseointegration. *Clin Oral Implan Res* 16: 657–666.
16. Gittens RA, McLachlan T, Olivares-Navarrete R, et al. (2011) The effects of combined micron-/submicron-scale surface roughness and nanoscale features on cell proliferation and differentiation. *Biomaterials* 32: 3395–3403.
17. Rupp F, Scheideler L, Olshanska N, et al. (2006) Enhancing surface free energy and hydrophilicity through chemical modification of microstructured titanium implant surfaces. *J Biomed Mater Res A* 76: 323–334.
18. Cai K, Bossert J, Jandt KD (2006) Does the nanometre scale topography of titanium influence protein adsorption and cell proliferation? *Colloid Surface B* 49: 136–144.
19. Migita S, Okuyama S, Araki K (2016) Sub-micrometer scale surface roughness of titanium reduces fibroblasts function. *J Appl Biomat Funct Mater* 14: e65–e69.
20. Chen CS, Mrksich M, Huang S, et al. (1997) Geometric control of cell life and death. *Science* 276: 1425–1428.
21. Chen CS, Mrksich M, Huang S, et al. (1998) Micropatterned surfaces for control of cell shape, position, and function. *Biotechnol Progr* 14: 356–363.

22. Chen CS, Alonso JL, Ostuni E, et al. (2003) Cell shape provides global control of focal adhesion assembly. *Biochem Bioph Res Co* 307: 355–361.
23. Gregory CA, Gunn WG, Peister A, et al. (2004) An alizarin red-based assay of mineralization by adherent cells in culture: comparison with cetylpyridinium chloride extraction. *Anal Biochem* 329: 77–84.
24. Damsky CH (1999) Extracellular matrix-integrin interactions in osteoblast function and tissue remodeling. *Bone* 25: 95–96.
25. Anselme K (2000) Osteoblast adhesion on biomaterials. *Biomaterials* 21: 667–681.
26. Boudreau NJ, Jones PL (1999) Extracellular matrix and integrin signaling: the shape of things to come. *Biochem J* 339: 481–488.
27. Geiger B, Spatz JP, Bershadsky AD (2009) Environmental sensing through focal adhesions. *Nat Rev Mol Cell Bio* 10: 21–33.
28. Wozniak MA, Modzelewska K, Kwong L, et al. (2004) Focal adhesion regulation of cell behavior. *BBA Mol Cell Res* 1692: 103–119.

AIMS Press